MIT Joint Program on the Science and Policy of Global Change

Climatology and Trends in the Forcing of the Stratospheric Zonal-Mean Flow

Erwan Monier and Bryan C. Weare

Report No. 190
January 2011

The MIT Joint Program on the Science and Policy of Global Change is an organization for research, independent policy analysis, and public education in global environmental change. It seeks to provide leadership in understanding scientific, economic, and ecological aspects of this difficult issue, and combining them into policy assessments that serve the needs of ongoing national and international discussions. To this end, the Program brings together an interdisciplinary group from two established research centers at MIT: the Center for Global Change Science (CGCS) and the Center for Energy and Environmental Policy Research (CEEPR). These two centers bridge many key areas of the needed intellectual work, and additional essential areas are covered by other MIT departments, by collaboration with the Ecosystems Center of the Marine Biology Laboratory (MBL) at Woods Hole, and by short- and long-term visitors to the Program. The Program involves sponsorship and active participation by industry, government, and non-profit organizations.

To inform processes of policy development and implementation, climate change research needs to focus on improving the prediction of those variables that are most relevant to economic, social, and environmental effects. In turn, the greenhouse gas and atmospheric aerosol assumptions underlying climate analysis need to be related to the economic, technological, and political forces that drive emissions, and to the results of international agreements and mitigation. Further, assessments of possible societal and ecosystem impacts, and analysis of mitigation strategies, need to be based on realistic evaluation of the uncertainties of climate science.

This report is one of a series intended to communicate research results and improve public understanding of climate issues, thereby contributing to informed debate about the climate issue, the uncertainties, and the economic and social implications of policy alternatives. Titles in the Report Series to date are listed on the inside back cover.

Ronald G. Prinn and John M. Reilly
Program Co-Directors

For more information, please contact the Joint Program Office

Postal Address: Joint Program on the Science and Policy of Global Change
77 Massachusetts Avenue
MIT E19-411
Cambridge MA 02139-4307 (USA)

Location: 400 Main Street, Cambridge
Building E19, Room 411
Massachusetts Institute of Technology

Access: Phone: +1(617) 253-7492
Fax: +1(617) 253-9845
E-mail: globalchange@mit.edu
Web site: http://globalchange.mit.edu/

Printed on recycled paper

Climatology and Trends in the Forcing of the Stratospheric Zonal-Mean Flow

Erwan Monier* and Bryan C. Weare†

Abstract

The momentum budget of the Transformed Eulerian-Mean (TEM) equation is calculated using the European Centre for Medium-Range Weather Forecasts (ECMWF) Re-Analysis (ERA-40). This study outlines the considerable contribution of the dissipative forcing, identified as a gravity wave drag, to the forcing of the zonal-mean flow. A trend analysis shows that, in recent times, the onset and break down of the Northern Hemisphere (NH) stratospheric polar night jet occur later. This temporal shift is associated with long-term changes in the planetary wave activity that are mainly due to synoptic waves. In the Southern Hemisphere (SH), the polar vortex shows a tendency to persist further into the SH summertime. This is explained by a statistically significant decrease in the intensity of the stationary EP flux divergence over the 1980–2001 period. The prevailing theory explaining the long-term changes in the stratospheric polar vortex postulates that ozone depletion leads to a strengthening of westerly winds which in turn causes the reduction in wave activity in high latitudes. We show that the strongest component in the dynamical response to stratospheric ozone changes is in fact the feedback of planetary wave activity on the zonal wind. Finally, we identify long-term changes in the Brewer-Dobson circulation that are mainly caused by trends in the planetary wave activity during winter and by trends in the gravity wave body force otherwise.

Contents

1. INTRODUCTION

Understanding stratospheric dynamics, its variability and interaction with photochemical processes has become increasingly important for the climate community. In the last decade, there has been growing evidence that the stratosphere can significantly influence the tropospheric weather and climate (Haynes, 2005). Baldwin and Dunkerton (2001) found that large circulation

* MIT Joint Program on the Science and Policy of Global Change, Cambridge, MA (E-mail: emonier@mit.edu).

† Atmospheric Science Program, Department of Land, Air and Water Resources, University of California, Davis.

anomalies in the lower stratosphere precede tropospheric anomalies in the Arctic and North Atlantic Oscillations, and in the location of storm tracks. Therefore, variations in the general circulation of the stratosphere could provide additional tropospheric extended-range forecasting skills (Baldwin and Dunkerton, 2001; Kuroda, 2008). There are many theories describing how the stratosphere can impact the troposphere, such as the downward reflection of wave flux (Perlwitz and Harnik, 2003) or the downward control (Song and Robinson, 2004). (Hartley *et al.*, 1998; Black, 2002) have shown that any change in the potential vorticity (PV) in the lower stratosphere induces instantaneous changes in wind and temperature at the tropopause that lead to feedbacks on the troposphere. Also, several studies reveal that the Arctic Oscillation (AO) can propagate downward from the stratosphere to the troposphere (Baldwin and Dunkerton, 1999; Kuroda and Kodera, 1999, 2004; Limpasuvan *et al.*, 2005). Finally, Ineson and Scaife (2009) show that the stratosphere plays a significant role in the European climate response to El Niño-Southern Oscillation (ENSO). For these reasons, a comprehensive understanding of the stratospheric dynamics variability and its causes is necessary in order to fully appreciate the potential impact of the stratosphere on climate change.

In addition, several studies have shown that the stratospheric dynamics have undergone significant changes in the last few decades. The Southern Hemisphere (SH) stratosphere exhibits a trend towards stronger westerly winds in the summer-fall season, producing a delay in the breakup of the polar vortex (Thompson and Solomon, 2002; Renwick, 2004). Karpetchko *et al.* (2005) show that wave forcing is not responsible for this long-term change and the trend is mainly attributed to Antarctic ozone depletion. As ozone loss in the polar region leads to an enhanced meridional temperature gradient near the subpolar stratosphere, it also results in the strengthening of westerly winds through thermal wind balance. Likewise, long-term trends in the Northern Hemisphere (NH) stratospheric dynamics have been identified. Hu and Tung (2003) detect a significant decline in wave activity in the higher latitudes, which starts from the early 1980s and exists only in late winter and springtime. This is consistent with the findings of Karpetchko and Nikulin (2004) who show a decrease in the vertical propagation of waves into the NH stratosphere in January and February. Additionally, Karpetchko and Nikulin (2004) reveal an increase in vertical propagation of waves in November and December. A study of the long-term changes in stratospheric wave activity by Kanukhina *et al.* (2008) indicates an intensification in the stationary planetary wave number 1 activity in the lower stratosphere polar region over the last 40 years. Hu and Tung (2003) propose a similar mechanism as in the SH whereby ozone depletion induces stronger westerly winds which refract planetary waves toward low latitudes and cause the reduction in wave activity in high latitudes. However, Karpetchko and Nikulin (2004) do not find any statistically significant trend in the winter zonal winds. Thus, there is still a lot of uncertainty in the source and the mechanism responsible for the various trends seen in the stratospheric dynamics.

The aim of this study is to investigate the role of the dynamical forcing in driving the stratospheric zonal-mean flow and its long-term changes, using a thorough budget analysis of the Transformed-Eulerian Mean (TEM) formulation of the momentum equation with the European

Centre for Medium-Range Weather Forecasts (ECMWF) Re-Analysis (ERA-40). The TEM formulation offers a useful diagnostic to interpret the forcing of the zonal-mean flow by eddies (Andrews *et al.*, 1983). This work provides a deeper look into the contribution of planetary waves, their stationary and transient components, as well as gravity waves, to the forcing of the stratospheric zonal-mean zonal wind and the residual mean meridional circulation. Such analysis is vital as the impacts of ozone depletion and wave activity variability on the long-term changes in stratospheric dynamics are not yet fully understood. This paper is organized as follows. The data, the equations and the basic description of the various eddy flux terms involved in the TEM formulation are briefly introduced in Section 2. Section 3 provides the results of the budget analysis of the climatology and trends of the stratospheric zonal-mean flow and its dynamical forcing. Finally, the discussion and concluding remarks are presented in Section 4.

2. DATA AND METHODOLOGY

2.1 Data

In this study, we use the six-hourly ERA-40 re-analysis (Uppala *et al.*, 2005) in order to calculate the various terms involved in the Transformed Eulerian-Mean formulation of the momentum equation. These terms include flux quantities like the Eliassen-Palm flux and the residual mean meridional circulation. The ERA-40 was chosen because it provides a complete set of meteorological data, over the whole globe on a 2.5° x 2.5° grid and over a large time period (1957–2001). Several studies have demonstrated the quality and usefulness of the ERA-40 data in the stratosphere. The annual cycle of the lower stratosphere in the ERA-40 compares well with other re-analysis datasets and the ERA-40 representation of the QBO is excellent up to 10 hPa (Pascoe *et al.*, 2005). The monthly mean ERA-40 temperatures and zonal winds in the lower stratosphere compare well with the NCEP-National Center for Atmospheric Research (NCAR) reanalysis-1 after 1979 (Karpetchko *et al.*, 2005). In addition, Knudsen *et al.* (2004) show that winter-averaged polar stratospheric cloud (PSC) areas in the NH, obtained from the ERA-40 and from the Free University of Berlin (FUB) analysis, which is largely independent of satellite data, agree well in most years. The ERA-40 dataset shows several weaknesses, such as an enhanced Brewer-Dobson circulation (van Noije *et al.*, 2004; Uppala *et al.*, 2005) or vertically oscillating stratospheric temperature biases over the Arctic since 1998 and over the Antarctic during the whole period (Randel *et al.*, 2004). Also, the ERA-40 re-analysis is unrealistic in the SH stratosphere during the pre-satellite era (Renwick, 2004; Karpetchko *et al.*, 2005). Nonetheless, the ERA-40 re-analysis provides a reasonably reliable dataset in the lower stratosphere during the satellite era. For this reason, the climatological analysis of the wave forcing of the stratospheric zonal-mean flow is performed over the years 1980 to 2001 and for pressure levels up to 10 hPa. Finally, the National Oceanic and Atmospheric Administration (NOAA) interpolated Outgoing Longwave Radiation (OLR) daily dataset (Liebmann and Smith, 1996) is used as a proxy for convection.

2.2 Methodology

2.2.1 Transformed Eulerian-Mean formulation

This study uses the Transformed Eulerian-Mean (TEM) formulation of the momentum equation in log-pressure and spherical coordinates in order to accurately diagnose the eddy forcing of the stratospheric zonal-mean flow. In spherical geometry, the TEM zonal momentum equation is (based on Equation 3.5.2a from Andrews *et al.* (1987)):

$$\underbrace{\frac{\partial \overline{u}}{\partial t}}_{\textit{Momentum tendency}} = \underbrace{f\overline{v}^{\star}}_{\textit{Coriolis force}} \underbrace{-\frac{\overline{v}^{\star}}{a\cos\phi}\frac{\partial}{\partial\phi}\left(\overline{u}\cos\phi\right) - \overline{w}^{\star}\overline{u}_z}_{\textit{Advective terms}} + \underbrace{\frac{1}{\rho_0 a\cos\phi}\nabla\cdot\vec{F}}_{\textit{EP flux divergence}} + \underbrace{\overline{X}}_{\textit{Residual term}} \tag{1}$$

In **Equation 1** and in the following equations, u is the zonal wind and the terms $\overline{v}^{\star}$, $\overline{w}^{\star}$ are, respectively, the horizontal and vertical components of the residual mean meridional circulation defined by (Equations 3.5.1a and 3.5.1b from Andrews *et al.* (1987)):

$$\overline{v}^{\star} = \overline{v} - \frac{1}{\rho_0}\frac{\partial}{\partial z}\left(\rho_0\frac{\overline{v'\theta'}}{\overline{\theta}_z}\right) \tag{2}$$

$$\overline{w}^{\star} = \overline{w} + \frac{1}{a\cos\phi}\frac{\partial}{\partial\phi}\left(\cos\phi\frac{\overline{v'\theta'}}{\overline{\theta}_z}\right) \tag{3}$$

where the overbars and primes indicate respectively the zonal means and departures from the zonal mean. θ is the potential temperature, v is the meridional wind and w is the vertical wind. $\nabla\cdot\vec{F}$ is the divergence of the Eliassen-Palm (EP) flux vector and represents the divergence of the eddy heat and eddy momentum fluxes. The EP flux vector $\vec{F}$ is defined by (Equations 3.5.3a and 3.5.3b from Andrews *et al.* (1987)):

$$\vec{F}^{(\phi)} = \rho_0 a\cos\phi\left(\overline{u}_z\frac{\overline{v'\theta'}}{\overline{\theta}_z} - \overline{v'u'}\right) \tag{4}$$

$$\vec{F}^{(z)} = \rho_0 a\cos\phi\left[\left(f - \frac{1}{a\cos\phi}\frac{\partial}{\partial\phi}\left(\overline{u}\cos\phi\right)\right)\frac{\overline{v'\theta'}}{\overline{\theta}_z} - \overline{w'u'}\right] \tag{5}$$

Finally, $\overline{X}$ represents unspecified horizontal components or friction or other dissipative mechanical forcing (such as gravity wave drag), which is calculated as the residual of the other terms.

Dunkerton (1978) showed that the Brewer-Dobson circulation should be interpreted as a Lagrangian mean circulation and could be approximated by the residual mean meridional circulation of the TEM equations. As a result, the residual mean meridional circulation is often used as a diagnostics for the Brewer-Dobson circulation (Callaghan and Salby, 2002; Nikulin and Karpechko, 2005; Miyazaki and Iwasaki, 2005; Eichelberger and Hartmann, 2005). Thus the

various processes forcing the zonal momentum tendency that are investigated in this study are separated into four categories: the Coriolis force due to the Brewer-Dobson circulation, the advection of zonal momentum by the Brewer-Dobson circulation, the divergence of the EP flux or planetary wave forcing, and the dissipative forcing. Additionally, from here on, when we refer to the EP flux divergence, or $\nabla \cdot \vec{F}$, we indicate the EP flux forcing term in Equation 1, including the weight by the density, the Earth's radius and cosine of latitude. The signs shown in Equation 1 are included in the various displayed terms. Each term is calculated using the six-hourly ERA-40 dataset. Finally, all derivatives are computed using centered finite differences.

2.2.2 Stationary and transient components

Because stratospheric dynamics are primarily driven by planetary waves, whether directly or indirectly, it is useful to decompose the zonal momentum forcing into contributions from stationary and transient waves. Stationary planetary waves are excited by the orography (Charney and Eliassen, 1949), especially in the NH, as well as by land-sea heating contrasts, which vary on the season time scale. Planetary transient waves, on the other hand, have smaller time scales ranging from a few days to a couple weeks and dominate synoptic weather patterns. The stationary components are computed by averaging temperature and wind fields over a month and then calculating the various terms of the TEM formulation. Once the stationary component is removed from the total term, which is calculated every six hours, only the contribution from the transient waves is left (Madden and Labitzke, 1981).

3. CLIMATOLOGY OF THE STRATOSPHERIC ZONAL-MEAN FLOW

3.1 Seasonal cycle of the zonal momentum budget

Figure 1 presents the annual cycle of the zonal-mean zonal wind, its tendency and forcing terms, averaged between 100 and 10 hPa for the 1980–2001 period. The annual cycle of the zonal flow shows distinct and well-known features such as the wintertime stratospheric polar night jets, strongest in the SH, and the latitudinal migration of the stratospheric tropical easterlies with the seasons (Oort, 1983; Andrews *et al.*, 1987; McWilliams, 2006). In the NH, the maximum in the stratospheric polar vortex westerlies occurs between December and February and is centered on 60°N, while weak easterlies are present from May to July. In the SH, the maximum in the westerlies occurs later in the winter than in the NH, between July and September, and is centered on 60°S. The zonal momentum tendency displays a clear seasonal cycle in the NH with an increase from July until December and a decrease from January until June with two distinct peaks (in the polar region and in the subtropics). In the SH, the momentum tendency presents a more complex structure with an increase lasting longer than in the NH, from January until August and a brief and intense decrease from September to December taking place mainly in the midlatitudes and polar region.

The Coriolis force due to the Brewer-Dobson circulation is characterized by a westward forcing all year long except right along the Equator where its forcing is close to zero. The Coriolis force displays a pronounced seasonal cycle in the NH with a broad maximum in the midlatitudes from November to January and a minimum in June and July. In the SH, the Coriolis

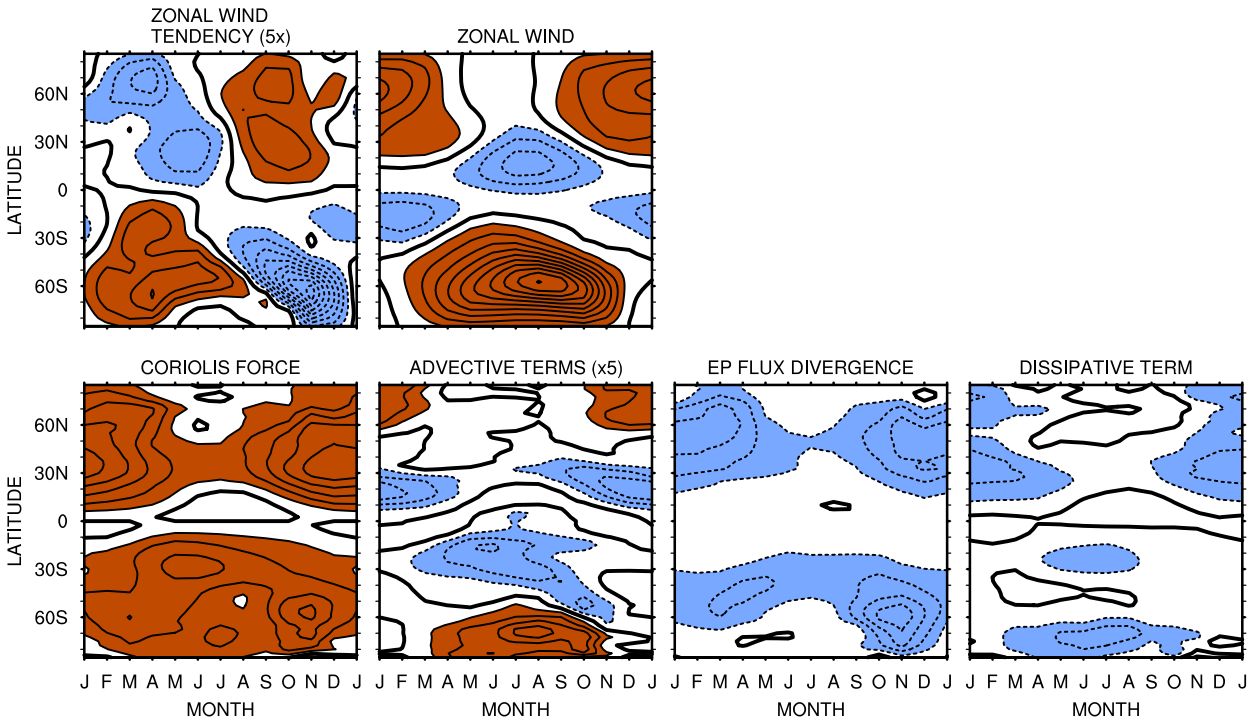

Figure 1. Annual cycle of the stratospheric zonal wind, zonal wind tendency and each forcing term in the TEM momentum equation averaged between 100 and 10 hPa. Dashed (solid) lines and blue (brown) colors represent negative (positive) values while the bold solid line represent the zero-line. Contour spacing is 6 m s^{-1} for the zonal wind and 0.5 m s^{-1} day^{-1} for the zonal wind tendency. Note that the zonal wind tendency and advective terms are weak compared to the other terms and are therefore multiplied by 5.

forcing presents two distinct peaks, weaker than in the NH, a brief and sharp maximum centered on 60°S from October to December and the other in the subtropics from May to July. Although much weaker than the other forcing terms, the advection of zonal momentum by the Brewer-Dobson circulation shows a clear seasonal annual cycle with the strongest forcing occurring in the wintertime. The advective terms correspond to a westward forcing in the polar region and an eastward forcing in the tropics in both SH and NH. The EP flux divergence consists of a continuous eastward forcing, strongest in the midlatitudes and present in both hemispheres. Like the Coriolis force, the EP flux divergence experiences a broad maximum from early winter until late spring in the NH and a sharp and brief peak in spring in the SH. Finally, the dissipative term contributes to a westward forcing during wintertime in the subtropics and polar regions.

The fact that the forcing of the stratospheric zonal wind takes place mainly in wintertime, particularly in the NH, is consistent with the finding of Charney and Drazin (1961) who showed that planetary Rossby waves can only propagate upward toward the stratosphere when the zonal wind is westerly but not too strong, which occurs in the wintertime in the NH. In the SH winter, the westerly winds are much stronger than in the NH and as a result they inhibit the vertical propagation of planetary waves into the stratosphere. This leads to a delay in the forcing of the stratospheric zonal wind. The EP flux divergence, which represents the westward force on the

zonal-mean flow due to vertically propagating planetary waves breaking and dissipating into the stratosphere, is primarily responsible for the deceleration of the polar night jets. This deceleration is partially balanced by the Coriolis force due to the Brewer-Dobson circulation. While the advective terms have small magnitudes compared to the EP flux and Coriolis terms, they have the same magnitude as the zonal momentum tendency and thus cannot be entirely neglected. Finally, the dissipative forcing displays magnitudes similar to the EP flux term, particularly in the NH wintertime, and thus contribute to breaking down the polar night jets.

3.2 Vertical structure of the zonal momentum budget

An example of the vertical structure of the zonal-mean zonal wind, its tendency and forcing terms for the months of January-February-March (JFM) in the NH, when the polar vortex is breaking down, is presented in **Figure 2**. The mean zonal winds exhibit strong westerlies in the subtropical lower stratosphere, corresponding to the top of the subtropical jet stream, and in the upper stratosphere over the subpolar region, where the stratospheric polar night jet is located. At the same time, the zonal momentum tendency acts to decelerate the strong westerlies in the polar region, leading to the break down of the polar vortex. Figure 2 shows that the EP flux divergence is negative over the whole region, with the strongest deceleration in the subtropical lower

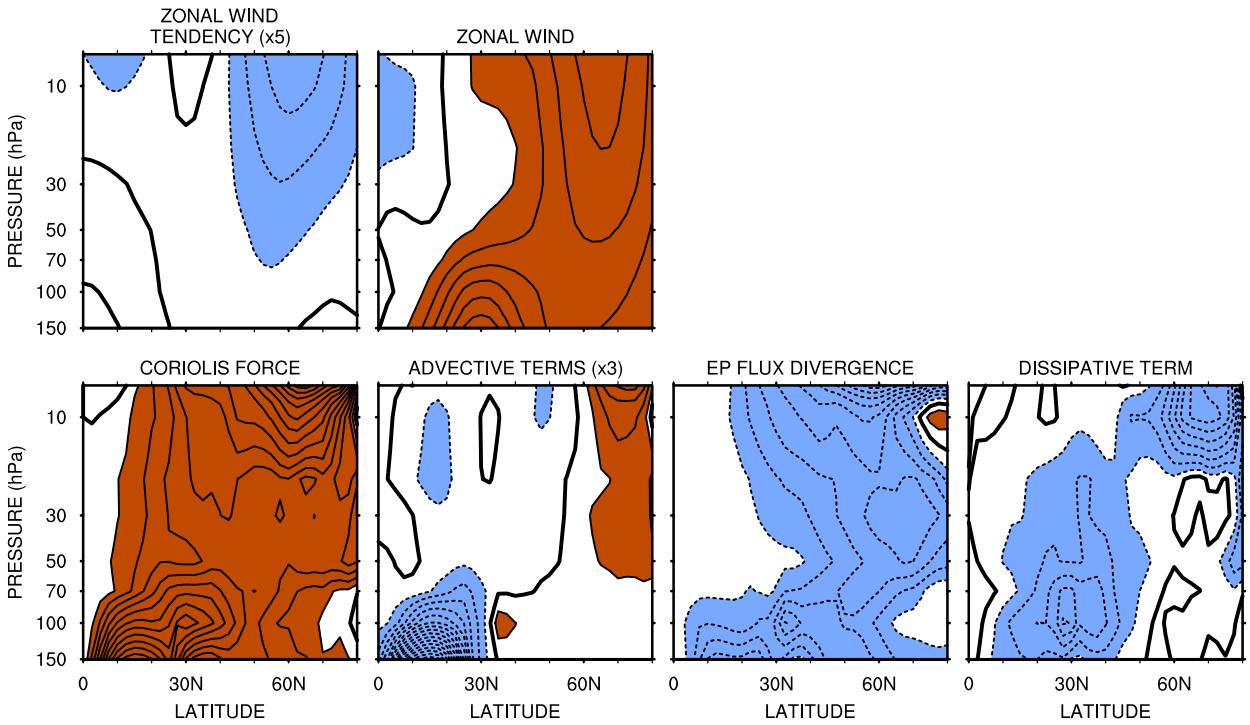

Figure 2. Zonal-mean zonal wind, zonal wind tendency and its forcing terms in the NH averaged over JFM 1980–2001. Dashed (solid) lines and blue (brown) colors represent negative (positive) values while the bold solid line represent the zero-line. Contour interval is 0.5 m s^{-1} day^{-1} for the mean zonal wind tendency and the forcing terms and 6 m s^{-1} for the mean zonal wind. Note that the zonal wind tendency and advective terms are weak compared to the other terms and are therefore multiplied by respectively 5 and 3.

stratosphere and subpolar upper stratosphere, and is largely balanced by the Coriolis force. The relatively small impact of the advective terms is mainly confined to the upper stratosphere in the polar region and to the tropics below 70 hPa. Finally, the dissipative forcing presents a clear deceleration in the latitude band between 20-40°N centered around 100 hPa with a maximum of around 2 m s^{-1}. It also shows a strong deceleration in the upper stratosphere polar region which reaches values larger than 3 m s^{-1} near 10 hPa. The magnitudes of these values confirm that the dissipative term plays a role in the momentum budget and thus requires a careful interpretation.

3.3 Dissipative term

The dissipative forcing consists of friction and any wave forcing not included in the divergence of the EP flux, such as gravity wave drag or wave breaking. Although many studies crudely parameterize the effects of wave dissipation using a simple Rayleigh friction coefficient (Schoeberl and Strobel, 1978; Holton and Wehrbein, 1980; Seol and Yamazaki, 1999), thus assuming a deceleration linear to the mean zonal wind, Shepherd and Shaw (2004) found that a Rayleigh friction introduces a nonphysical momentum sink. Also, according to Haynes (2005), it is difficult to argue that such a friction is at all relevant in the stratosphere. This budget analysis reveals that the dissipative term shows similarities in sign and structure to a Rayleigh friction but that its magnitude is one order magnitude too large to be explained by friction (if assuming a Rayleigh friction coefficient of 1/(80 days) in the stratosphere like in Holton and Wehrbein (1980)). Furthermore, the patterns of the dissipative forcing in this study are similar to the structure of orographic gravity wave drag reported in several studies. For example, a January simulation of orographic gravity wave drag in the Canadian Middle Atmosphere Model (CMAM) shows a deceleration of 2-3 m s^{-1} day^{-1} centered around 100 hPa in the latitude band between 30-50°N (McFarlane, 2000). Such gravity wave drag in the subtropical region is in reasonable agreement with similar studies (Palmer *et al.*, 1986) and radar measurements (Fritts and Alexander, 2003). In addition, the CMAM simulation also shows a gravity wave drag in the upper stratosphere, with maximum deceleration close to 5 m s^{-1} day^{-1} above 10 hPa at midlatitudes and near the polar region. Therefore, the dissipative term in the subtropics, mid-latitudes and in the polar region seems a reasonable representation of the orographic gravity wave drag. In the ERA-40, the influence of subgrid-scale orography on the momentum of the atmosphere is represented by a combination of lower-troposphere drag created by orography and vertical profiles of drag due to the absorption and reflection of vertically propagating gravity waves generated by stably stratified flow over the subgrid-scale orography. The scheme is described in detail in Lott and Miller (1997).

Figure 3 shows a vertical cross-section of the dissipative term in the tropics for the months of January and July, as well as its annual cycle superposed onto OLR anomalies. The dissipative forcing exhibits positive values near the Equator for both months, corresponding to westerly acceleration. Since the prevailing winds are easterly in the tropical region, the dissipative forcing decelerates the zonal-mean zonal wind. In January, the drag force is located south of the Equator and reaches 0.4 m s^{-1} day^{-1} above 100 hPa while it is located north of the Equator in July and

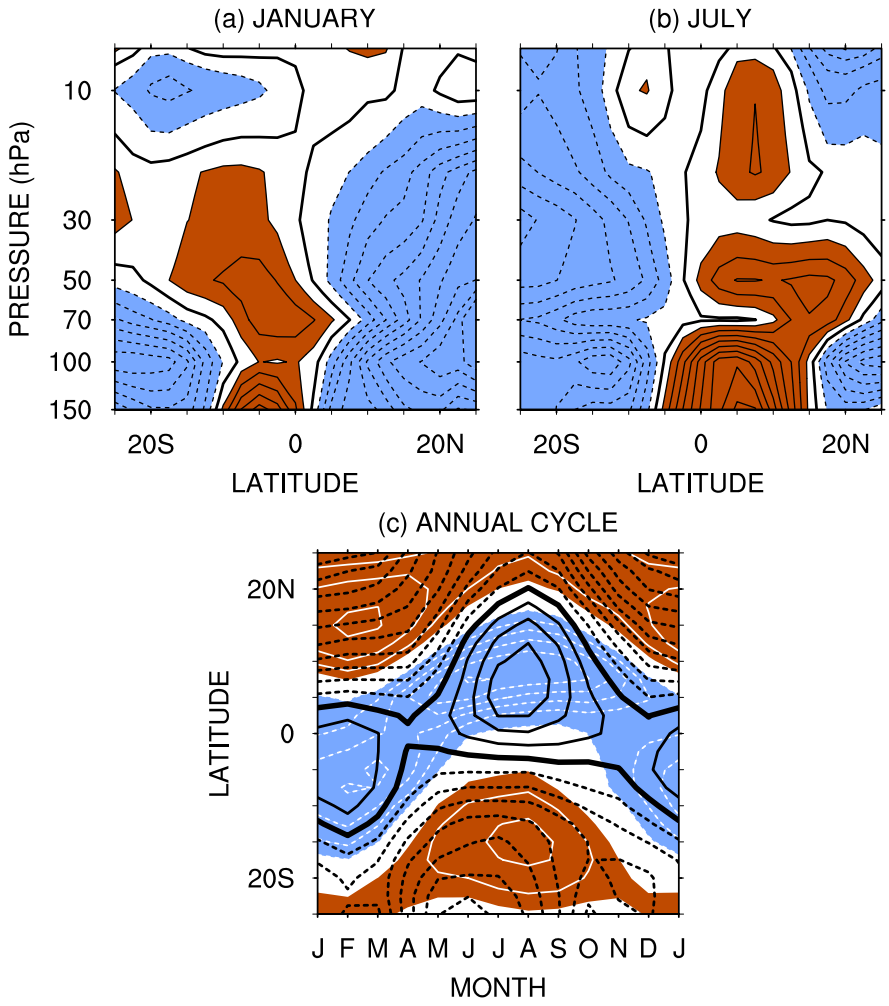

Figure 3. Latitude-height cross-section of the dissipative term in the TEM momentum equation for (a) January and (b) July. Dashed (solid) lines and blue (brown) colors represent negative (positive) values while the bold solid line represent the zero-line. Contour interval is 0.1 m s^{-1} day^{-1}. (c) Annual cycle of the dissipative term (*black contour lines*) overlaid on the OLR departures from the annual mean averaged between 25°S-25°N (*color shading with white contour lines*). Dashed (solid) black lines represent negative (positive) values while the bold solid line represent the zero-line for the dissipative term. Blue (brown) colors with dashed (solid) white lines represent negative (positive) values for the OLR. Contour interval is 0.1 m s^{-1} day^{-1} for the dissipative term and 5 W m^{-2} for the OLR.

shows stronger accelerations, reaching up to 0.5 m s^{-1} day^{-1}. These results are similar to zonal-mean zonal wind tendency due to the gravity wave drag forced by subgrid-scale cumulus convection in the National Center for Atmospheric Research Community Climate Model (NCAR CCM3) presented by Chun *et al.* (2004). The seasonal cycle of the dissipative forcing displays a migration of the westerly acceleration with latitude across the Equator between boreal and austral summers that mirrors that of OLR. In effect, the dissipative forcing over the tropics exhibits westerly acceleration following the Inter-Tropical Convergence Zone (ITCZ), with magnitudes consistent with a gravity wave drag forced by convection. This confirms that the dissipative term displays the characteristics of a gravity wave drag, whether forced by orography or convection.

3.4 EP flux term

While the dissipative term seems to contribute to the break down of the polar vortex, the main forcing in the deceleration of the zonal wind in the NH wintertime is the EP flux divergence. An example of the vertical structure of the EP flux vector, the EP flux divergence and its horizontal and vertical components for JFM is shown in **Figure 4**. A distinct property of the EP flux divergence is the competition between its two components, which largely cancel each other in the extratropics. $\nabla \cdot \vec{F}^{(\phi)}$ is dominated by the horizontal divergence of the meridional eddy momentum flux and $\nabla \cdot \vec{F}^{(z)}$ is controlled by the vertical divergence of the meridional eddy heat flux (Andrews *et al.*, 1987). Figure 4 underlines the fact that while the eddy momentum flux and eddy heat flux have opposite contributions, they do not act separately but in combination, with a net impact resulting in a westward body force that breaks down the polar vortex in the NH wintertime. In addition, the presence of a greater land area and topography distribution in the NH results in a stronger contribution from stationary processes, which are forced by topography and land-sea heating contrasts. The main difference between the stationary and transient components resides in the presence of a distinct divergence of the transient EP flux in the polar region upper stratosphere. While considerable divergence of EP flux can happen during sudden stratospheric warming events (Palmer, 1981), it is unclear why it is removed from the climatology mean.

Under the WKBJ (Wentzel-Kramers-Brillouin-Jeffreys) approximation and when dealing with planetary waves with small latitudinal and vertical wavelength, it can be shown that the EP flux vector is proportional to the local group velocity projected onto the meridional plane (Edmon Jr *et al.*, 1980). Thus, $\vec{F}$ can be thought as a diagnostic tool for the net propagation of energy by planetary waves from one region, at one latitude and one height, to another. Figure 4 indicates that, in the NH wintertime, the vertical component of the EP flux vector, dominated by the meridional eddy heat flux, is oriented upward and decreases with height, leading to a net convergence. In other words, as Rossby planetary waves propagate upward into the stratosphere, their energy weakens with height through dissipation. Concurrently, the horizontal component of the EP flux vector shows that planetary waves propagating into the stratosphere are bent away from the stratospheric polar night jet toward the Equator at midlatitudes and toward the pole in the lower stratosphere polar region, leading to a strong divergence of the meridional eddy momentum flux superposed onto the location of the strong westerlies. Consequently, the cancellation between the components of the EP flux divergence is the result of the refraction of planetary waves around the stratospheric polar night jet. Indeed, the effective index of refraction for the planetary waves depends primarily on the distribution of the zonal mean wind with height and energy can be reflected in regions where the zonal wind is westerly and large, like the stratospheric polar night jet (Charney and Drazin, 1961).

A similar analysis of the EP flux terms for the SH reveals that the main difference between the two hemispheres is the stronger contribution of transient wave forcing. The contribution of stationary processes is mostly limited to the polar region, where the presence of the asymmetric Antarctic topography and ice-sea heating contrasts drives stationary wave activity (Parish *et al.*, 1994; Lachlan-Cope *et al.*, 2001).

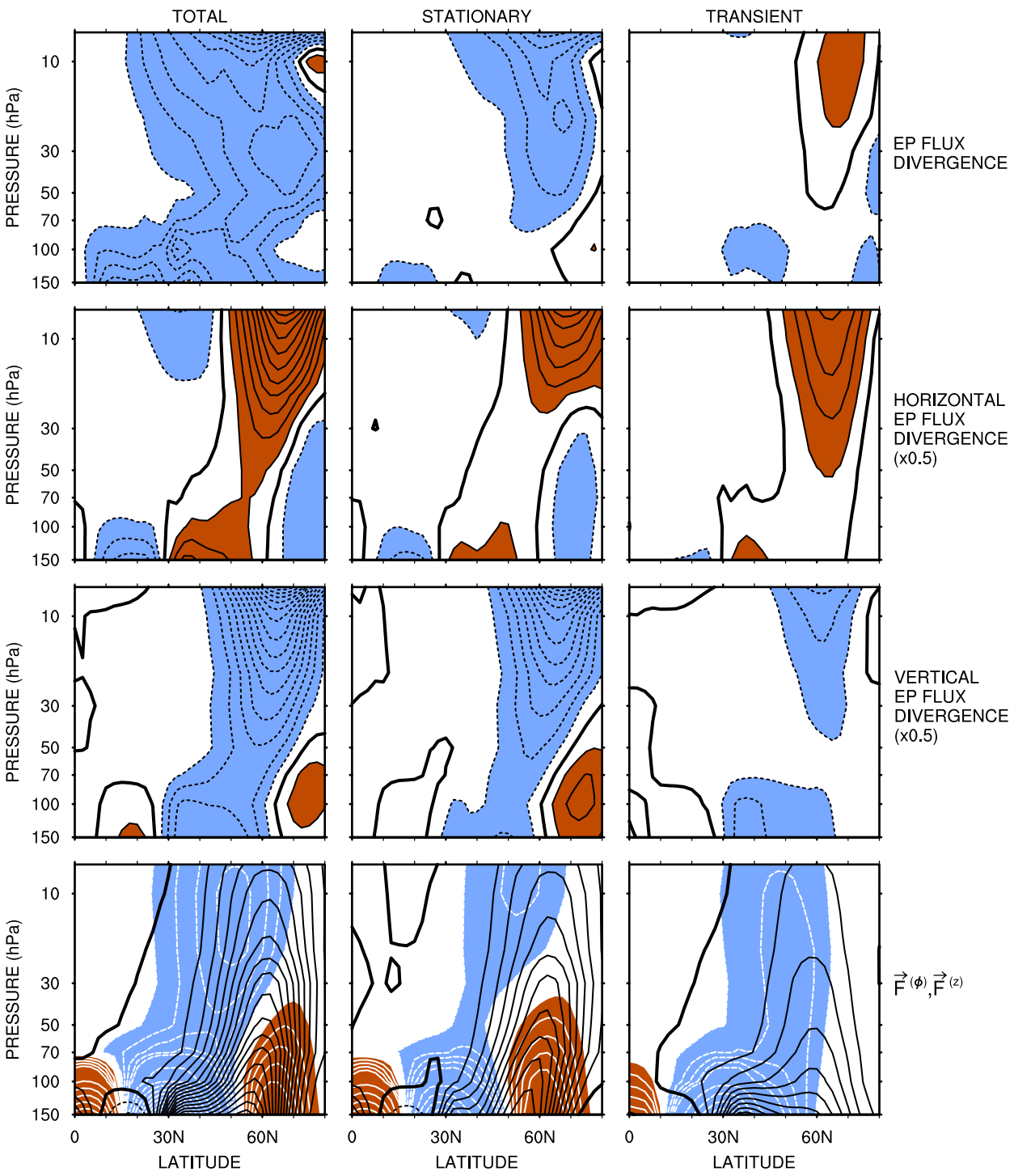

Figure 4. Same as Figure 2 but for the EP flux divergence, its horizontal and vertical components, and the EP flux vector, including stationary and transient components. Blue (brown) colors with dashed (solid) white lines represent negative (positive) values for $\vec{F}^{(\phi)}$. Dashed (solid) black lines represent negative (positive) values while the bold solid line represent the zero-line for $\vec{F}^{(z)}$. Contour spacing is 0.5 m s^{-1} day^{-1} for the EP flux divergence and its horizontal and vertical components, 10^6 kg s^{-2} for $\vec{F}^{(\phi)}$ until 5x10^6 kg s^{-2} and 5x10^6 kg s^{-2} above, and 10^4 kg s^{-2} for $\vec{F}^{(z)}$. Note that the horizontal and vertical components of the EP flux divergence are large compared to the EP flux divergence and are therefore multiplied by 0.5.

3.5 Correlations of zonal momentum forcing

To gain more insight into the relative contribution of the forcing terms to the zonal wind variability, spatial correlation coefficients between the forcing terms are calculated and shown in **Figure 5**. This analysis is similar to the statistics presented in Pfeffer (1992), but is extended to a 22-year daily climatology, includes an analysis of the stratosphere and focuses only on one hemisphere at a time to account for the strong seasonality of the wave-mean flow interaction in the stratosphere. Figure 5 reveals that, in the troposphere, the spatial correlation coefficients have little seasonal variability. Overall, the tropospheric zonal momentum tendency is highly correlated with $\nabla \cdot \vec{F}^{(\phi)}$ but not with $\nabla \cdot \vec{F}^{(z)}$. Meanwhile, the Coriolis and advective terms exhibit a high negative correlation with $\nabla \cdot \vec{F}^{(z)}$, reflecting the fact that the wave drag exerted by $\nabla \cdot \vec{F}^{(z)}$ is consumed by driving the Brewer-Dobson circulation, thereby negating its effect on the eddy-induced momentum tendency. Even though the horizontal EP flux is much smaller than its vertical component in the troposphere, it explains most of the temporal variability of the mean zonal flow. This fact is due to the latitudinal and vertical distribution of the stratification parameter that gives more weight to the forcing by the divergence of the horizontal EP flux than to the forcing by the vertical EP flux (Pfeffer, 1987). In the troposphere, $\nabla \cdot \vec{F}^{(z)}$ and $\nabla \cdot \vec{F}^{(\phi)}$ have very different impacts on the mean zonal flow and are not at all correlated.

In the stratosphere, the correlation coefficients present a strong seasonality due to the absence of planetary wave propagation into the stratosphere at midlatitudes in summer. As a result, the contribution of the sum of the Coriolis, advective and dissipative terms to the zonal momentum tendency is very strong in the summertime, with correlation above 70%. $\nabla \cdot \vec{F}^{(\phi)}$ and $\nabla \cdot \vec{F}^{(z)}$ present a moderate anti-correlation, implying they act in combination. As a result, the momentum tendency is more correlated to $\nabla \cdot \vec{F}$ than to each of its components. This analysis identifies the more intricate role of the vertical EP flux divergence in driving the zonal current in the stratosphere. The correlation between the momentum tendency and $\nabla \cdot \vec{F}$ is strongest in March, when it reaches 50%. Finally, unlike in the troposphere, the Coriolis and advective terms are poorly correlated with $\nabla \cdot \vec{F}^{(z)}$ or even $\nabla \cdot \vec{F}$. Instead they show a high negative correlation with the dissipative term, which corresponds to gravity wave activity. Therefore, this analysis suggests that, in the Northern Hemisphere, gravity waves may play an equally large role as planetary waves in driving the Brewer-Dobson circulation. The same correlation analysis was done to the Southern Hemisphere and yields similar results so the same interpretation can be applied to the stratospheric wave forcing in the SH.

An alternative explanation for the strong anti-correlation between the dissipative term and the Coriolis and advective terms is the Brewer-Dobson circulation, which has a strong bias all year long in the ERA-40 (van Noije *et al.*, 2004; Uppala *et al.*, 2005). When calculating the dissipative term as the residual of the other forcing terms, a bias in the Brewer-Dobson circulation could lead to an artificial bias of opposite sign in the residual term, resulting in a strong anti-correlation between both terms. However, since the structure and magnitude of the dissipative term are consistent with a gravity wave drag, any bias introduced by the Brewer-Dobson circulation seems to be weak. For this reason, we consider in the following work that the dissipative term is indeed

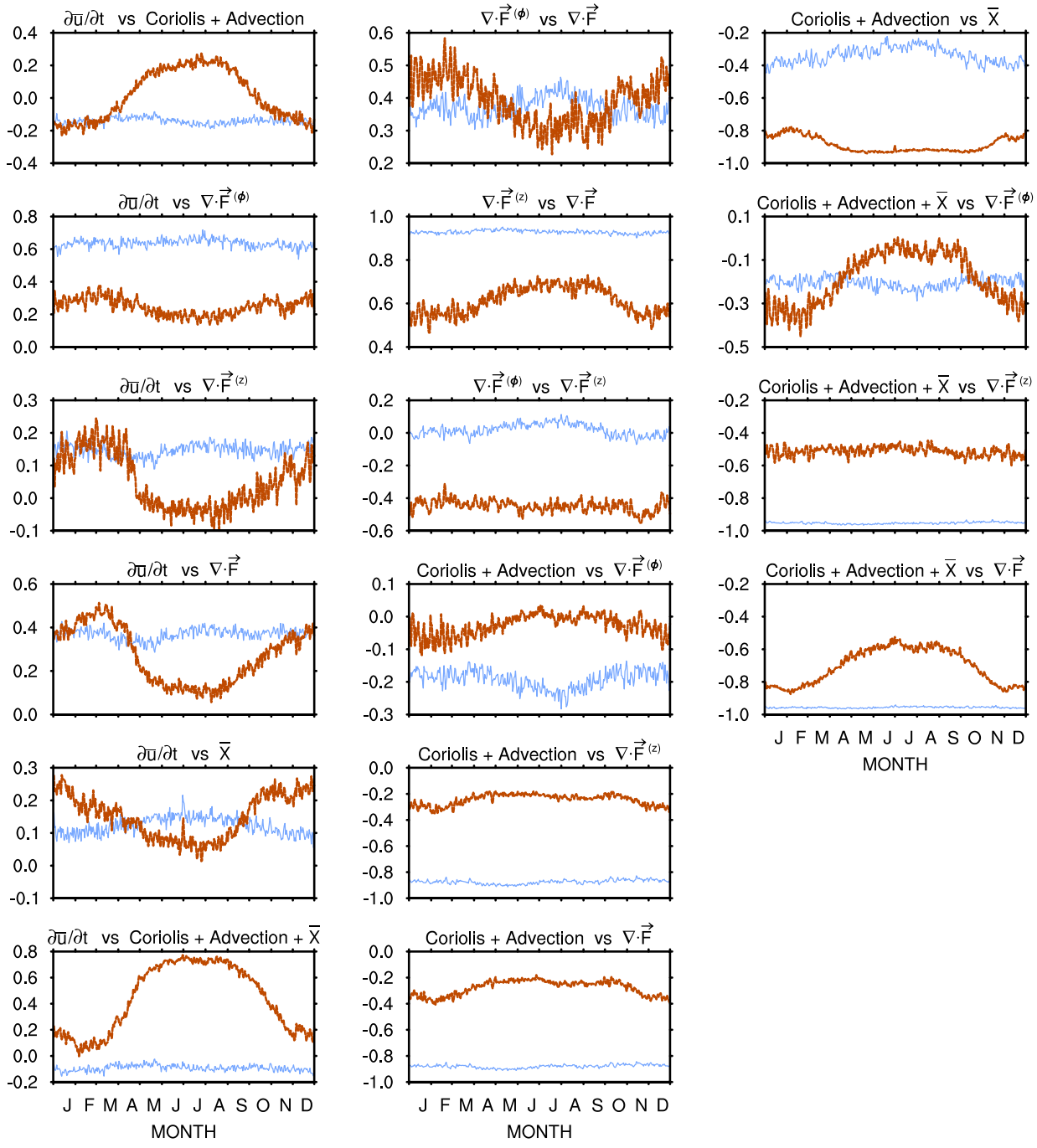

Figure 5. Time variations of spatial correlations over the Northern Hemisphere in the troposphere (blue lines), up to 250 hPa, and in the stratosphere (brown lines), between 150 and 10 hPa, between the different terms and their components of the TEM momentum equation. Correlation coefficients were calculated every 6 hours over the time period 1 Jan 1980–31 Dec 2001.

representative of the gravity wave activity.

4. TRENDS IN THE WAVE FORCING OF THE STRATOSPHERIC ZONAL-MEAN MOMENTUM

4.1 Zonal-mean zonal wind

The long-term trends and interannual variability of the lower and middle stratosphere zonal-mean zonal wind are investigated in **Figure 6**. The variances and trends are calculated after the zonal-mean zonal wind is averaged between 100 and 10 hPa. The zonal wind displays a large variance, representing its interannual variability, in the tropics all year long that corresponds to the Quasi-Biennial Oscillation (QBO). The tropical variability shows a maximum in variance during the NH late spring, which is consistent with the fact that the onset of both easterly and westerly QBO phases occurs mainly during NH late spring at the 50 hPa level (Dunkerton, 1990; Baldwin *et al.*, 2001). Since the period of the QBO is variable and because the duration of each phase at any level is long compared with the transition time, the strongest variability tends to occur near the phase transition. Outside of the tropics, the zonal wind variance is large in the polar region and is associated with the breakdown of the polar night jet, from early winter until early spring in the NH and limited to the late spring in the SH. The trend analysis reveals a long-term increase in the SH zonal wind from November until January, indicating that the SH polar vortex tends to persist longer in recent summers than in the earlier part of the record. In particular, the SH zonal wind has increased in December at a rate of 3.5 m s^{-1} per decade and at a 99% significance level (calculated using a Student's t-test). This result is in agreement with

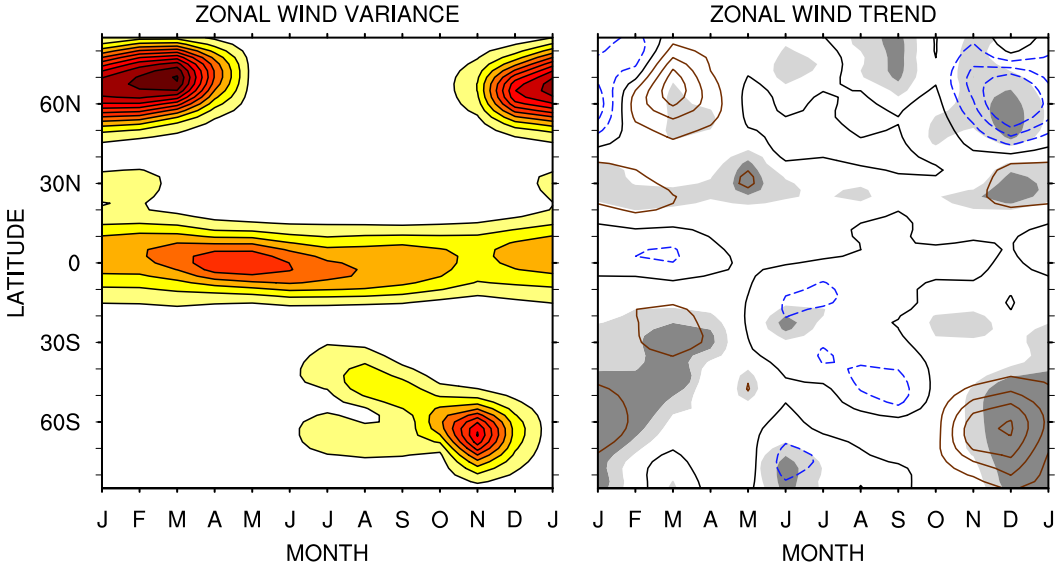

Figure 6. Annual cycle of the zonal wind sample variance and trend. The variances and trends are calculated after the zonal wind is averaged between 100 and 10 hPa. Dashed blue (solid brown) lines represent negative (positive) values while the bold solid line represents the zero-line. Light grey (dark grey) shading represents the 85% (95%) statistical significance level of the trends. Contour spacing is 10 m^2 s^{-2} for the variance and 1 m s^{-1} per decade for the trend.

several studies (Thompson and Wallace, 2000; Thompson and Solomon, 2002; Renwick, 2004; Karpetchko *et al.*, 2005). Several recent years (1998, 1999 and 2001) display strong westerlies close to 10 m s^{-1} in December, compared to the 22-year mean which is close to zero. In the NH, a clear and significant negative trend in the zonal wind is present in the late fall and early winter while positive trends occur during the breakdown. This indicates a temporal shift in the timing of the NH polar vortex which is pushed further into the winter. In December, the zonal wind has weakened at a rate of over 4 m s^{-1} per decade, with a 95% statistical significance level. Meanwhile the March westerlies have strengthened, at a rate close to 3 m s^{-1} per decade, with a 87% significance level. While that trend shows a moderate statistical significance in this analysis, it is similar to results by Thompson and Wallace (2000) who show that the westerlies near 55°N have increased by as much as 10 m s^{-1} over 30 years (1968-1997) at 50 hPa. The modest statistical significance found in this work is likely due to the averaging done over pressure levels.

4.2 Wave forcing of zonal momentum budget

Figure 7 shows the annual cycle of the linear trends over 1980–2001 of the momentum tendency and its forcing terms. In the NH, positive trends in the Coriolis and advective terms are present from April until November and are largely balanced by opposite trends in the dissipative terms. In winter, the Coriolis and advective terms experience negative trends that are offset by positive trends in the EP flux divergence, which correspond to a long-term weakening of the planetary wave activity. The intensification of the Brewer-Dobson circulation seen in spring, summer and fall is consistent with the response to a doubled CO_2 climate (Eichelberger and Hartmann, 2005; Butchart *et al.*, 2006; Haklander *et al.*, 2008) and appears to be primarily driven

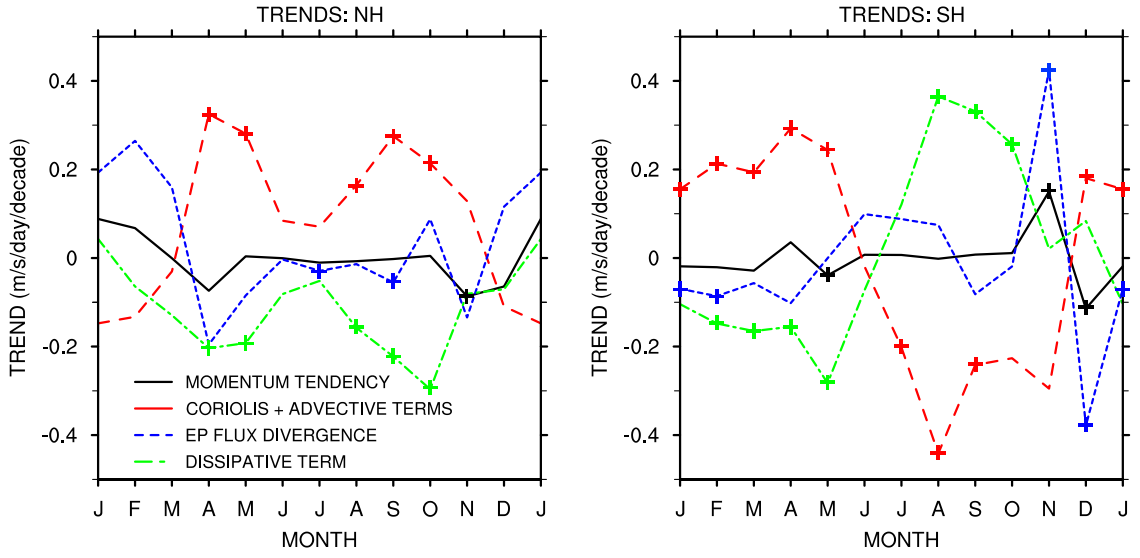

Figure 7. Annual cycle of the trends in the momentum tendency and its forcing terms, for the (left) NH and the (right) SH. The trends are calculated after the momentum tendency and its forcing terms are averaged between 100 and 10 hPa and between 50°-70°. Trends that are statistically significant at the 90% level are indicated with a cross.

by long-term changes in the gravity wave drag. The temporal shift in the polar vortex can be attributed to a decrease in the EP flux in late fall and winter, followed by an increase in early spring. The trends in the planetary wave forcing precede the trends in the zonal wind by one month, showing causality. In November, the EP flux divergence has decreased at a rate of $0.15\,\mathrm{m\,s^{-1}\,day^{-1}}$ per decade and a significance level of 82% while it has increased in February at a rate of $0.21\,\mathrm{m\,s^{-1}\,day^{-1}}$ per decade and significance level of 70%. These weak levels of significance are possibly due to the large averaging area (100 to 10 hPa and 50°-70°) so that further analysis without the averaging is necessary to determine whether the trends in the planetary wave activity are real or not. In the SH, the Coriolis and advective terms exhibit positive trends in summer and fall and negative trends elsewhere. Like in the NH, these long-term changes are largely balanced by trends of opposite signs in the dissipative forcing, except when the trends in the EP flux divergence are large (in November and December). The persistence of the polar vortex in the SH late spring can be explained by a significant trend in the zonal momentum tendency in November associated with a long-term weakening of the wave activity. In November, the EP flux divergence has decreased at a rate of $0.46\,\mathrm{m\,s^{-1}\,day^{-1}}$ per decade at the 97.5% statistical significance level. While Karpetchko *et al.* (2005) find no decrease in the heat flux and conclude that the planetary wave forcing is not responsible for the more persistent polar vortex, they solely focus on the month of October. This analysis shows that a weakening in the planetary forcing does indeed take place, but in the month of November. While the trends in the Coriolis and advective terms mirror that of the dissipative term over most of the year in both hemispheres, they do not during the NH winter and during the SH late spring. This further demonstrates that the relationship between the Brewer-Dobson circulation and the dissipative term is not constrained by an artificial bias due to the enhancement of the Brewer-Dobson circulation, which is present all year long in the ERA-40. Instead, it points toward a physical interaction where gravity wave drag plays a significant role in driving the residual mean meridional circulation when the planetary wave activity is weak.

Figure 8 shows latitude-height cross-sections of the trends in the EP flux vector and its divergence in the SH for the month of November, with the contribution of stationary and transient waves. It indicates a strong and significant decrease in the intensity of the EP flux divergence in the polar region between 100 and 10 Pa, statistically significant at the 90% level. In addition, the trends in the vertical component of the EP flux demonstrates that significantly less energy is being transported vertically into the stratospheric polar region by planetary waves, especially by stationary waves. Meanwhile, trends in the horizontal component of the EP flux are weak and not significant. A similar analysis is done for the month of February in the NH and shown in **Figure 9**. A significant decrease in the strength of the EP flux divergence is present in the subpolar and polar region below 100 hPa and above 20 hPa with competing contribution from stationary (intensification) and transient (weakening) waves. Overall, the trend analysis of the EP flux divergence is noisy and does not paint a clear picture. However, the EP flux vector exhibits more distinct patterns. Significantly less energy is transported vertically into the stratosphere by transient waves in the later years. Meanwhile a positive trend in the vertical component of the

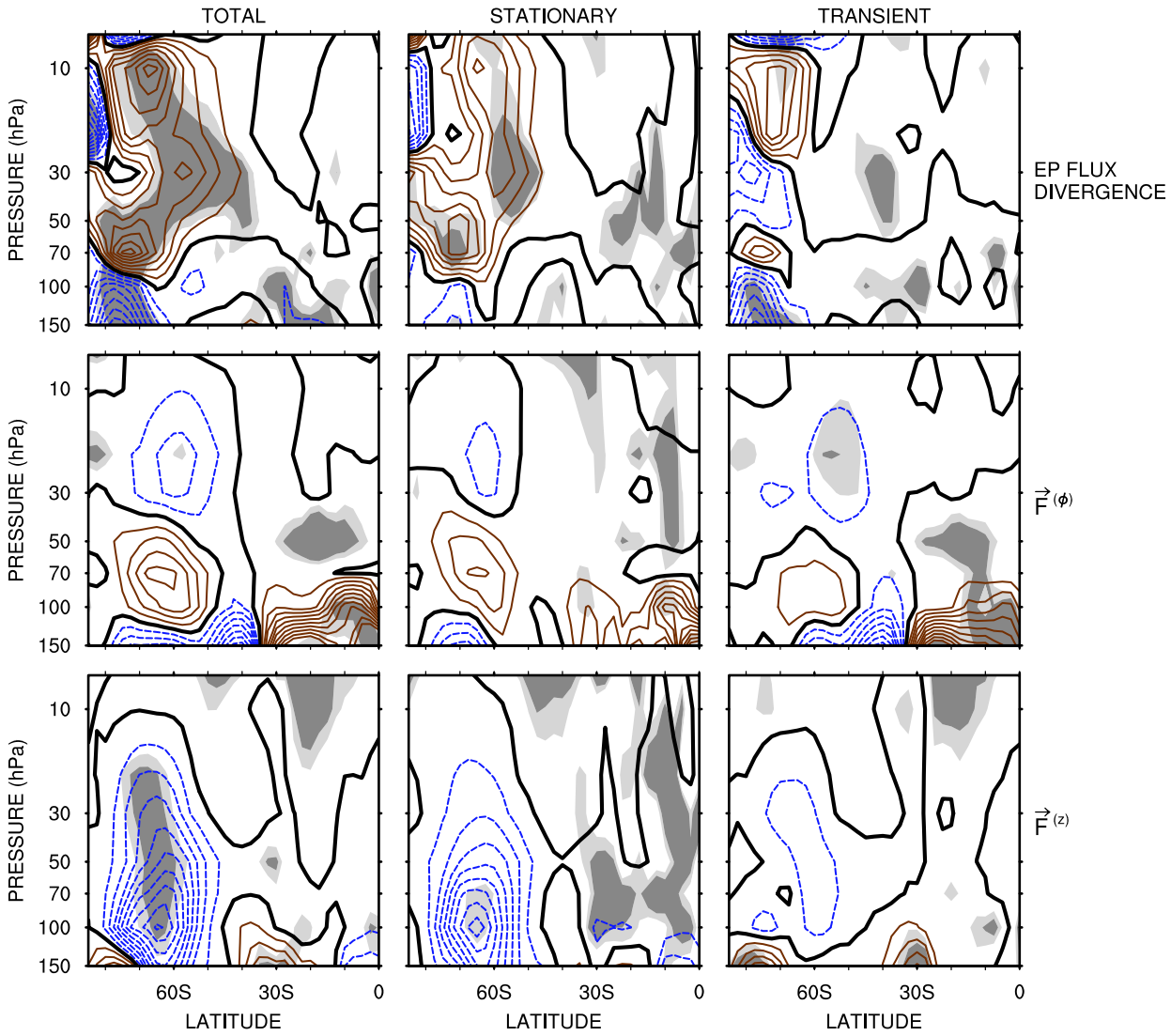

Figure 8. Trends in the EP flux vector and its divergence, including stationary and transient components, for the month of November in the SH. Dashed (solid) lines represent negative (positive) values while the bold solid line represent the zero-line. Light blue (light brown) color represents the 80% statistical significance level of negative (positive) trends. Dark blue (dark brown) color represents the 90% statistical significance level of negative (positive) trends. Contour spacing is 0.2 m s^{-1} day^{-1} per decade for the EP flux divergence, 2x10^5 kg s^{-2} per decade for $\vec{F}^{(\phi)}$ and 2x10^3 kg s^{-2} per decade for $\vec{F}^{(z)}$.

stationary EP flux vector is present north of 60°, consistent with the findings of Kanukhina *et al.* (2008), but this trend is not statistically significant and thus should be disregarded. Moreover, this analysis shows a significant tendency toward more poleward refraction of stationary waves in the polar region and of transient waves at mid-latitudes. The study of the trends in the NH EP flux forcing for the month of November (not shown) reveals an increase in wave activity, which is statistically significant at midlatitudes and at several pressure levels in the polar region. This increase is principally due to transient waves propagating from the troposphere into the stratosphere significantly more in the later years. Concurrently, the equatorward refraction of

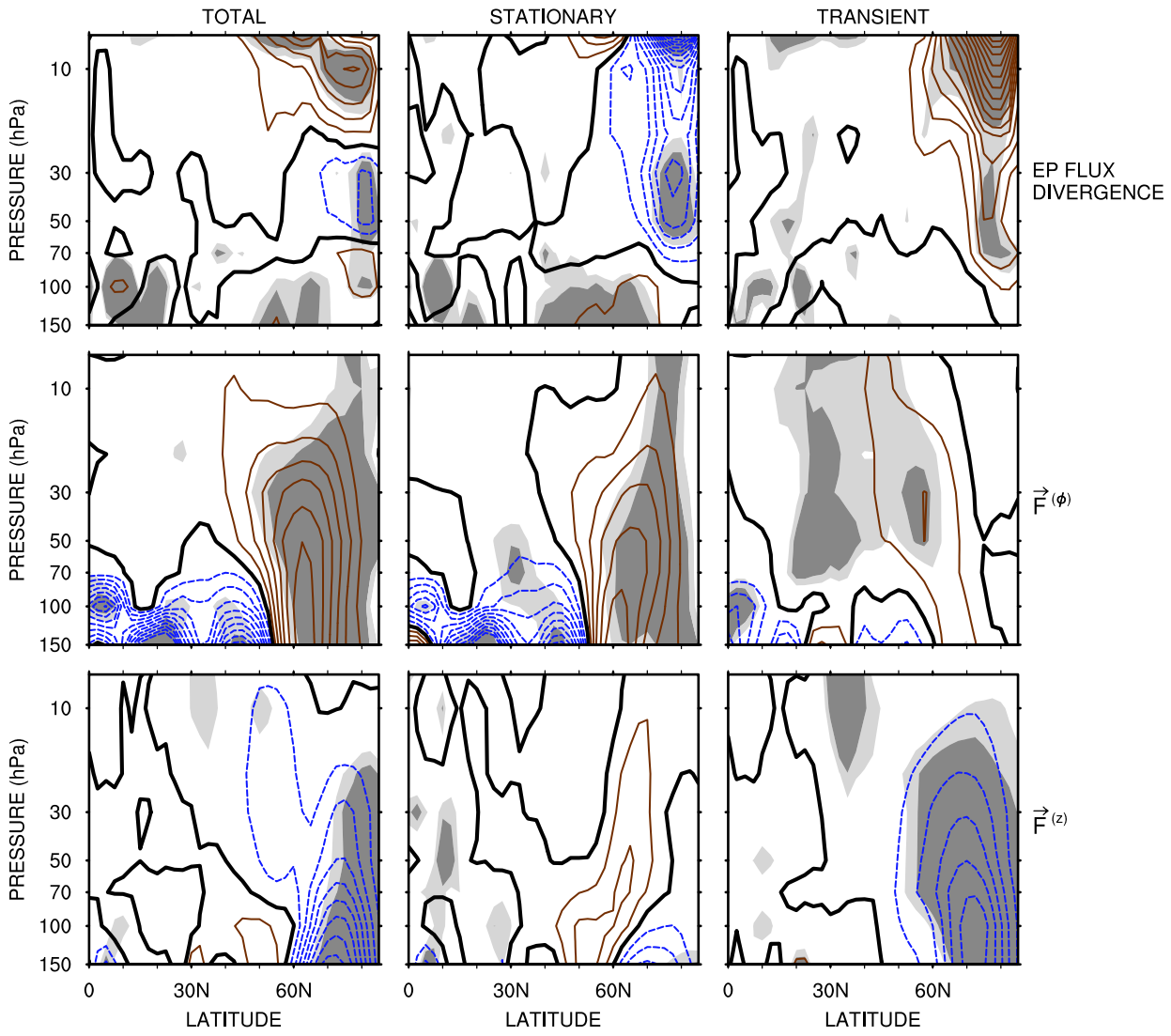

Figure 9. Same as Figure 8 but for the month of February in the NH. Contour spacing is 0.5 m s^{-1} day^{-1} per decade for the EP flux divergence, 5x10^5 kg s^{-2} per decade for $\vec{F}^{(\phi)}$ and 5x10^3 kg s^{-2} per decade for $\vec{F}^{(z)}$.

planetary waves is greatly increased.

The systematic analysis of trends in the EP flux vector and its divergence reveals tendencies consistent with that of the polar night jet. While the statistical significance and the contribution of the stationary and transient components differ between the two hemispheres, a significant decrease in the planetary wave activity occurs one month before the strongest and most significant positive trend in the zonal-mean zonal wind that correspond to a delay in the breakdown of the polar vortex. Also, in the NH early winter, an increase in planetary wave activity is followed, a month later as well, by a decrease in the strength of the polar vortex. Finally, the increase and decrease of wave activity in the NH early winter and late winter, respectively, are very similar in nature while simply opposite in sign.

5. DISCUSSION AND CONCLUSION

A careful analysis of the budget of the TEM momentum equation in the ERA-40 re-analysis was carried out. It provides further insight into the role of the planetary wave and gravity wave forcing on the stratospheric zonal-mean flow. The resolved terms in the momentum equation are the zonal momentum tendency, the Coriolis force and advective terms due to the Brewer-Dobson circulation, and the Eliassen-Palm flux divergence, which is a measure of the planetary wave forcing. In addition, a dissipative forcing term is calculated as the residual term in the TEM momentum equation. The climatology of the resolved forcing terms is consistent with the wave-mean flow interaction theory, as the EP flux divergence contributes to the breakdown of the polar vortex while being balanced by the Coriolis force due to the Brewer-Dobson circulation. In addition, the dissipative forcing displays the correct features of a gravity wave drag, including location, seasonality and magnitude compared to model simulations and measurements. As a result, the momentum budget based on the TEM framework presented in this study provides a reasonable method to investigate the dynamical forcing in the stratosphere over the whole globe and over long time periods using re-analysis datasets. The momentum budget outlines the considerable contribution of the dissipative forcing in driving the stratospheric circulation, as it exhibits magnitudes similar to that of the EP flux divergence in some regions of the stratosphere. Gravity waves may play an equally large role as planetary waves in driving the Brewer-Dobson circulation, especially during spring, summer and fall. Therefore, the gravity wave drag should not be entirely dismissed from research related to the wave forcing of the stratospheric dynamics.

The trend analysis shows that there is a statistically significant weakening of the Northern Hemisphere stratospheric polar night jet in December and a moderately significant strengthening in March, hinting at a delay of the breakdown of the polar vortex. Both changes in the strength of the westerly winds follow changes in the planetary wave activity, mainly due to transient waves, with a delay of one month. This is consistent with the findings of Karpetchko and Nikulin (2004) who observed a decrease in the heat flux in January and February in the NCEP-NCAR-reanalysis. In their study, Karpetchko and Nikulin (2004) fail to link the trend in the wave activity to changes in the zonal-mean zonal wind because they only investigate trends in the polar night jet at the same period, and not a month later. This underlines the importance of a thorough analysis of the seasonality of the long-term changes in the stratospheric dynamics. In the Southern Hemisphere, the polar vortex also shows a tendency to persist further into the SH summertime. This is explained by a statistically significant decrease in the intensity of the stationary EP flux divergence. Thus, the two hemispheres differ in the source of the decrease in wave activity: transient waves in the NH and stationary waves in the SH.

Several studies have attributed the delay in the breakdown of the SH polar vortex (Thompson and Solomon, 2002; Renwick, 2004) to ozone depletion. Weare (2009) showed that there is a distinct symmetric mode between the zonal wind and ozone in the SH and that this mode contains a clear long-term trend. Hu and Tung (2003) advance a mechanism whereby ozone depletion leads to an enhanced meridional temperature gradient near the subpolar stratosphere, strengthening westerly winds. The strengthened winds would then refract planetary waves toward

low latitudes and cause the reduction in wave activity in high latitudes. It is also possible that the ozone depletion directly impacts the vertical propagation of planetary waves and in turn the zonal wind, as suggested by the ozone-modified refractive index for vertically propagating planetary waves introduced by Nathan and Cordero (2007), which accounts for how ozone photochemistry, ozone transport, and Newtonian cooling can combine to modify wave propagation and drag on the zonal-mean flow. While the strongest ozone trends over Antarctica take place from September to November (Monier and Weare, 2010), the significant long-term changes in the zonal wind are limited to the months November, December and January. This indicates a delay of two months in the dynamical response of ozone depletion in the SH. The absence of any significant trends in the zonal wind in September and October can be explained by the absence of eddy feedback. During these months, the polar vortex is too strong to allow any vertical propagation of planetary waves into the stratosphere so that trends in the planetary wave forcing are suppressed. Meanwhile, in November when the polar vortex begins to break down, the vertically propagating waves can be modulated by the strength of the westerlies (associated with ozone depletion) and provide a strong positive feedback. In the NH, there is no delay between the ozone trend and the trends in the zonal wind because the the timing of the ozone depletion coincides with the break down of the polar vortex, in March (Monier and Weare, 2010). As a result, this analysis underlines the vital role of planetary wave feedback in the dynamical response to ozone changes in the stratosphere. Furthermore, this study shows that the dominant cause for the decrease in wave activity seems to be a reduction in the vertical propagation of planetary waves and not a meridional bending as proposed in Hu and Tung (2003). Especially, in the NH, the decrease in wave activity is associated with a tendency for more poleward refraction and not equatorward.

Finally, long-term changes in the residual mean meridional circulation were found in both hemispheres. In the NH, the Brewer-Dobson circulation significantly intensifies from spring to fall as a result of increasing gravity wave drag. In winter, the strength of the residual circulation weakens due to a decrease in the planetary wave activity. Meanwhile, the residual mean meridional circulation intensifies in the SH during summer and fall and weakens during winter and spring. These trends are driven by opposite trends in the dissipative term, except in November and December when the long-term changes in the planetary wave forcing are large. This is consistent with the fact that gravity wave driving is believed to dominate outside of the wintertime in the stratosphere, when the EP flux divergence is small (Fritts and Alexander, 2003). This underlines the considerable role of gravity waves in driving the Brewer-Dobson circulation and its long-term changes. This is on par with the findings of McLandress and Shepherd (2009) who show that parameterized orographic gravity wave drag account for 40% of the long-term trend in annual mean net upward mass flux at 70 hPa.

While many studies rely solely on planetary waves to explain the stratospheric dynamics, this budget analysis draws attention to the need to account for gravity waves. As a result, a strong emphasis should be put on developing models with strong capabilities to accurately simulate gravity waves, both orographic and convectively forced. There are many more issues that need to be addressed regarding long-term changes in the stratospheric dynamics. Since ozone depletion

can directly alter planetary wave activity in the stratosphere through ozone photochemistry, ozone transport, and Newtonian cooling, there is a need for more theoretical and applied studies to investigate these mechanisms. Similarly, the impact of climate change due to increasing anthropogenic emissions of greenhouse gas on the wave activity in the stratosphere needs to be better resolved. Finally, some limitations of the zonally-averaged framework are made clear in this study and it is perhaps time to expand such budget analysis using a 3D formulation of EP flux divergence and gravity wave drag.

Acknowledgements

The authors want to thank Professor Terrence R. Nathan for his advice on this project and Professor R. Alan Plumb for his comments, as well as the various anonymous reviewers for the helpful discussions. ERA-40 data were provided by the European Centre for Medium-Range Weather Forecasts from their website at http://data-portal.ecmwf.int/data/d/era40_daily/. Interpolated OLR data were provided by the NOAA/OAR/ESRL PSD, Boulder, Colorado, USA, from their website at http://www.esrl.noaa.gov/psd/. This study was partially supported by the National Science Foundation grant ATM0733698.

6. REFERENCES

Andrews, D. G., J. R. Holton and C. B. Leovy, 1987: *Middle Atmosphere Dynamics*. Academic Press, 489 p.

Andrews, D. G., J. D. Mahlman and R. W. Sinclair, 1983: Eliassen-Palm Diagnostics of Wave-Mean Flow Interaction in the GFDL "SKYHI" General Circulation Model. *J. Atmos. Sci.*, **40**(12): 2768–2784. doi:10.1175/1520-0469(1983)040<2768:ETWATM>2.0.CO;2.

Baldwin, M. P. and T. J. Dunkerton, 1999: Propagation of the Arctic Oscillation from the stratosphere to the troposphere. *J. Geophys. Res.*, **104**(D24): 30937–30946. doi:10.1029/1999JD900445.

Baldwin, M. P. and T. J. Dunkerton, 2001: Stratospheric Harbingers of Anomalous Weather Regimes. *Science*, **294**(5542): 581–584. doi:10.1126/science.1063315.

Baldwin, M. P., L. J. Gray, T. J. Dunkerton, K. Hamilton, P. H. Haynes, W. J. Randel, J. R. Holton, M. J. Alexander, I. Hirota, T. Horinouchi, D. B. A. Jones, J. S. Kinnersley, C. Marquardt, K. Sato and M. Takahashi, 2001: The Quasi-Biennial Oscillation. *Rev. Geophys.*, **39**(2): 179–229. doi:10.1029/1999RG000073.

Black, R. X., 2002: Stratospheric Forcing of Surface Climate in the Arctic Oscillation. *J. Climate*, **15**(3): 268–277. doi:10.1175/1520-0442(2002)015<0268:SFOSCI>2.0.CO;2.

Butchart, N., A. A. Scaife, M. Bourqui, J. de Grandpre, S. H. E. Hare, J. Kettleborough, U. Langematz, E. Manzini, F. Sassi, K. Shibata, D. Shindell and M. Sigmond, 2006: Simulations of anthropogenic change in the strength of the Brewer-Dobson circulation. *Clim. Dyn.*, **27**(7-8): 727–741. doi:DOI 10.1007/s00382-006-0162-4.

Callaghan, P. F. and M. L. Salby, 2002: Three-Dimensionality and Forcing of the Brewer–Dobson Circulation. *J. Atmos. Sci.*, **59**(5): 976–991. doi:10.1175/1520-0469(2002)059<0976:TDAFOT>2.0.CO;2.

Charney, J. G. and P. G. Drazin, 1961: Propagation of Planetary-Scale Disturbances from the Lower into the Upper Atmosphere. *J. Geophys. Res.*, **66**(1): 83–109. doi:10.1029/JZ066i001p00083.

Charney, J. G. and A. Eliassen, 1949: A numerical method for predicting the perturbations of the middle latitude westerlies. *Tellus*, **1**(2): 38–54. doi:10.1111/j.2153-3490.1949.tb01258.x.

Chun, H. Y., I. S. Song, J. J. Baik and Y. J. Kim, 2004: Impact of a Convectively Forced Gravity Wave Drag Parameterization in NCAR CCM3. *J. Climate*, **17**(18): 3530–3547. doi:10.1175/1520-0442(2004)017<3530:IOACFG>2.0.CO;2.

Dunkerton, T., 1978: On the Mean Meridional Mass Motions of the Stratosphere and Mesosphere. *J. Atmos. Sci.*, **35**(12): 2325–2333. doi:10.1175/1520-0469(1978)035<2325:OTMMMM>2.0.CO;2.

Dunkerton, T. J., 1990: Annual variation of deseasonalized mean flow acceleration in the equatorial lower stratosphere. *J. Meteor. Soc. Japan*, **68**(4): 499–508.

Edmon Jr, H. J., B. J. Hoskins and M. E. McIntyre, 1980: Eliassen-Palm Cross Sections for the Troposphere. *J. Atmos. Sci.*, **37**(12): 2600–2616. doi:10.1175/1520-0469(1980)037<2600:EPCSFT>2.0.CO;2.

Eichelberger, S. J. and D. L. Hartmann, 2005: Changes in the strength of the Brewer-Dobson circulation in a simple AGCM. *Geophys. Res. Lett.*, **32**: L15807. doi:10.1029/2005GL022924.

Fritts, D. C. and M. J. Alexander, 2003: Gravity wave dynamics and effects in the middle atmosphere. *Rev. Geophys.*, **41**(1): 1003. doi:10.1029/2001RG000106.

Haklander, A. J., P. C. Siegmund, M. Sigmond and H. M. Kelder, 2008: How does the northern-winter wave driving of the Brewer-Dobson circulation increase in an enhanced-CO2 climate simulation? *Geophys. Res. Lett.*, **35**: L07702. doi:10.1029/2007GL033054.

Hartley, D. E., J. T. Villarin, R. X. Black and C. A. Davis, 1998: A new perspective on the dynamical link between the stratosphere and troposphere. *Nature*, **391**(6666): 471–474. doi:10.1038/35112.

Haynes, P., 2005: Stratospheric Dynamics. *Annu. Rev. Fluid Mech.*, **37**: 263–293. doi:10.1146/annurev.fluid.37.061903.175710.

Holton, J. R. and W. M. Wehrbein, 1980: The Role of Forced Planetary Waves in the Annual Cycle of the Zonal Mean Circulation of the Middle Atmosphere. *J. Atmos. Sci.*, **37**(9): 1968–1983. doi:10.1175/1520-0469(1980)037<1968:TROFPW>2.0.CO;2.

Hu, Y. and K. K. Tung, 2003: Possible ozone-induced long-term changes in planetary wave activity in late winter. *J. Climate*, **16**(18): 3027–3038. doi:10.1175/1520-0442(2003)016<3027:POLCIP>2.0.CO;2.

Ineson, S. and A. A. Scaife, 2009: The role of the stratosphere in the European climate response to El Nino. *Nat. Geosci.*, **2**(1): 32–36. doi:10.1038/ngeo381.

Kanukhina, A. Y., E. V. Suvorova, L. A. Nechaeva, E. K. Skrygina and A. I. Pogoreltsev, 2008: Climatic variability of the mean flow and stationary planetary waves in the NCEP/NCAR reanalysis data. *Ann. Geophys.*, **26**(5): 1233–1241. doi:10.5194/angeo-26-1233-2008.

Karpetchko, A., E. Kyrö and B. M. Knudsen, 2005: Arctic and Antarctic polar vortices 1957-2002 as seen from the ERA-40 reanalyses. *J. Geophys. Res.*, **110**: D21109. doi:10.1029/2005JD006113.

Karpetchko, A. and G. Nikulin, 2004: Influence of early winter upward wave activity flux on midwinter circulation in the stratosphere and troposphere. *J. Climate*, **17**(22): 4443–4452. doi:10.1175/JCLI-3229.1.

Knudsen, B. M., N. R. P. Harris, S. B. Andersen, B. Christiansen, N. Larsen, M. Rex and B. Naujokat, 2004: Extrapolating future Arctic ozone losses. *Atmos. Chem. Phys.*, **4**: 1849–1856. doi:10.5194/acp-4-1849-2004.

Kuroda, Y., 2008: Role of the stratosphere on the predictability of medium-range weather forecast: A case study of winter 2003–2004. *Geophys. Res. Lett.*, **35**: L19701. doi:10.1029/2008GL034902.

Kuroda, Y. and K. Kodera, 1999: Role of planetary waves in the stratosphere-troposphere coupled variability in the northern hemisphere winter. *Geophys. Res. Lett.*, **26**(15): 2375–2378. doi:10.1029/1999GL900507.

Kuroda, Y. and K. Kodera, 2004: Role of the Polar-night Jet Oscillation on the formation of the Arctic Oscillation in the Northern Hemisphere winter. *J. Geophys. Res.*, **109**: D11112. doi:10.1029/2003JD004123.

Lachlan-Cope, T. A., W. M. Connolley and J. Turner, 2001: The Role of the Non-Axisymmetric Antarctic Orography in forcing the Observed Pattern of Variability of the Antarctic Climate. *Geophys. Res. Lett.*, **28**(21): 4111–4114. doi:10.1029/2001GL013465.

Liebmann, B. and C. A. Smith, 1996: Description of a Complete (Interpolated) Outgoing Longwave Radiation Dataset. *Bull. Amer. Meteor. Soc.*, **77**(6): 1275–1277.

Limpasuvan, V., D. L. Hartmann, D. W. J. Thompson, K. Jeev and Y. L. Yung, 2005: Stratosphere-troposphere evolution during polar vortex intensification. *J. Geophys. Res.*, **110**: D24101. doi:10.1029/2005JD006302.

Lott, F. and M. J. Miller, 1997: A new subgrid-scale orographic drag parametrization: Its formulation and testing. *Quart. J. Roy. Meteor. Soc.*, **123**(537): 101–127. doi:10.1002/qj.49712353704.

Madden, R. A. and K. Labitzke, 1981: A free Rossby wave in the troposphere and stratosphere during January 1979. *J. Geophys. Res.*, **86**(C2): 1247–1254. doi:10.1029/JC086iC02p01247.

McFarlane, N. A., 2000: Gravity-Wave Drag. In: *Numerical Modeling of the Global Atmosphere in the Climate System*, P. W. Mote and A. O'Neill, (eds.), Kluwer Academic Publishers, pp. 297–320.

McLandress, C. and T. G. Shepherd, 2009: Simulated Anthropogenic Changes in the Brewer-Dobson Circulation, Including Its Extension to High Latitudes. *J. Climate*, **22**(6): 1516–1540. doi:10.1175/2008JCLI2679.1.

McWilliams, J. C., 2006: *Fundamentals of Geophysical Fluid Dynamics*. Cambridge University Press, 266 p.

Miyazaki, K. and T. Iwasaki, 2005: Diagnosis of meridional ozone transport based on mass-weighted isentropic zonal means. *J. Atmos. Sci.*, **62**(4): 1192–1208. doi:10.1175/JAS3394.1.

Monier, E. and B. C. Weare, 2010: Climatology and Trends in the Wave Forcing of the Stratospheric Ozone Transport. *Atmos. Chem. Phys.*, submitted; see also MIT JPSPGC *Report 191* (http://globalchange.mit.edu/files/document/MITJPSPGC_Rpt191.pdf).

Nathan, T. R. and E. C. Cordero, 2007: An ozone-modified refractive index for vertically propagating planetary waves. *J. Geophys. Res.*, **112**: D02105. doi:10.1029/2006JD007357.

Nikulin, G. and A. Karpechko, 2005: The mean meridional circulation and midlatitude ozone buildup. *Atmos. Chem. Phys.*, **5**(11): 3159–3172. doi:10.5194/acp-5-3159-2005.

Oort, A. H., 1983: *Global atmospheric circulation statistics, 1958-1973*. Professional Paper 14. National Oceanic and Atmospheric Administration: Washington, D.C., 180 p.

Palmer, T. N., 1981: Diagnostic Study of a Wavenumber-2 Stratospheric Sudden Warming in a Transformed Eulerian-Mean Formalism. *J. Atmos. Sci.*, **38**(4): 844–855. doi:10.1175/1520-0469(1981)038<0844:DSOAWS>2.0.CO;2.

Palmer, T. N., G. J. Shutts and R. Swinbank, 1986: Alleviation of a systematic westerly bias in general circulation and numerical weather prediction models through an orographic gravity wave drag parametrization. *Quart. J. Roy. Meteor. Soc.*, **112**(474): 1001–1039. doi:10.1002/qj.49711247406.

Parish, T. R., D. H. Bromwich and R. Y. Tzeng, 1994: On the role of the Antarctic continent in forcing large-scale circulations in the high southern latitudes. *J. Atmos. Sci.*, **51**(24): 3566–3579. doi:10.1175/1520-0469(1994)051<3566:OTROTA>2.0.CO;2.

Pascoe, C. L., L. J. Gray, S. A. Crooks, M. N. Juckes and M. P. Baldwin, 2005: The quasi-biennial oscillation: Analysis using ERA-40 data. *J. Geophys. Res.*, **110**: D08105. doi:10.1029/2004JD004941.

Perlwitz, J. and N. Harnik, 2003: Observational Evidence of a Stratospheric Influence on the Troposphere by Planetary Wave Reflection. *J. Climate*, **16**(18): 3011–3026. doi:10.1175/1520-0442(2003)016<3011:OEOASI>2.0.CO;2.

Pfeffer, R. L., 1987: Comparison of conventional and transformed Eulerian diagnostics in the troposphere. *Quart. J. Roy. Meteor. Soc.*, **113**(475): 237–254. doi:10.1002/qj.49711347514.

Pfeffer, R. L., 1992: A Study of Eddy-induced Fluctuations of the Zonal-Mean Wind Using Conventional and Transformed Eulerian Diagnostics. *J. Atmos. Sci.*, **49**(12): 1036–1050. doi:10.1175/1520-0469(1992)049<1036:ASOEIF>2.0.CO;2.

Randel, W. J., P. Udelhofen, E. Fleming, M. Geller, M. Gelman, K. Hamilton, K. D., D. Ortland, S. Pawson, R. Swinbank, F. Wu, M. P. Baldwin, M. L. Chanin, P. Keckhut, K. Labitzke, E. Remsberg, A. J. Simmons and D. Wu, 2004: The SPARC Intercomparison of Middle-Atmosphere Climatologies. *J. Climate*, **17**(5): 986–1003. doi:10.1175/1520-0442(2004)017<0986:TSIOMC>2.0.CO;2.

Renwick, J. A., 2004: Trends in the Southern Hemisphere polar vortex in NCEP and ECMWF reanalyses. *Geophys. Res. Lett.*, **31**: L07209. doi:10.1029/2003GL019302.

Schoeberl, M. R. and D. F. Strobel, 1978: The Zonally Averaged Circulation of the Middle Atmosphere. *J. Atmos. Sci.*, **35**(4): 577–591. doi:10.1175/1520-0469(1978)035<0577:TZACOT>2.0.CO;2.

Seol, D. I. and K. Yamazaki, 1999: Residual mean meridional circulation in the stratosphere and upper troposphere: Climatological aspects. *J. Meteor. Soc. Japan*, **77**(5): 985–996.

Shepherd, T. G. and T. A. Shaw, 2004: The Angular Momentum Constraint on Climate Sensitivity and Downward Influence in the Middle Atmosphere. *J. Atmos. Sci.*, **61**(23): 2899–2908. doi:10.1175/JAS-3295.1.

Song, Y. and W. A. Robinson, 2004: Dynamical mechanisms for stratospheric influences on the troposphere. *J. Atmos. Sci.*, **61**(14): 1711–1725. doi:10.1175/1520-0469(2004)061<1711:DMFSIO>2.0.CO;2.

Thompson, D. W. J. and S. Solomon, 2002: Interpretation of recent Southern Hemisphere climate change. *Science*, **296**(5569): 895–899. doi:10.1126/science.1069270.

Thompson, D. W. J. and J. M. Wallace, 2000: Annular modes in the extratropical circulation. Part I: Month-to-month variability. *J. Climate*, **13**(5): 1000–1016. doi:10.1175/1520-0442(2000)013<1000:AMITEC>2.0.CO;2.

Uppala, S. M., P. W. Kallberg, A. J. Simmons, U. Andrae, V. D. Bechtold, M. Fiorino, J. K. Gibson, J. Haseler, A. Hernandez, G. A. Kelly, X. Li, K. Onogi, S. Saarinen, N. Sokka, R. P. Allan, E. Andersson, K. Arpe, M. A. Balmaseda, A. C. M. Beljaars, L. Van De Berg, J. Bidlot, N. Bormann, S. Caires, F. Chevallier, A. Dethof, M. Dragosavac, M. Fisher, M. Fuentes, S. Hagemann, E. Holm, B. J. Hoskins, L. Isaksen, P. A. E. M. Janssen, R. Jenne, A. P. McNally, J. F. Mahfouf, J. J. Morcrette, N. A. Rayner, R. W. Saunders, P. Simon, A. Sterl, K. E. Trenberth, A. Untch, D. Vasiljevic, P. Viterbo and J. Woollen, 2005: The ERA-40 re-analysis. *Quart. J. Roy. Meteor. Soc.*, **131**(612): 2961–3012. doi:DOI 10.1256/qj.04.176.

van Noije, T. P. C., H. J. Eskes, M. van Weele and P. F. J. van Velthoven, 2004: Implications of the enhanced Brewer-Dobson circulation in European Centre for Medium-Range Weather Forecasts reanalysis ERA-40 for the stratosphere-troposphere exchange of ozone in global chemistry transport models. *J. Geophys. Res.*, **109**: D19308. doi:10.1029/2004JD004586.

Weare, B. C., 2009: Dynamical modes associated with the Antarctic ozone hole. *Atmos. Chem. Phys.*, **9**(15): 5403–5416. doi:10.5194/acp-9-5403-2009.

REPORT SERIES of the MIT *Joint Program on the Science and Policy of Global Change*

1. **Uncertainty in Climate Change Policy Analysis** *Jacoby & Prinn* December 1994
2. **Description and Validation of the MIT Version of the GISS 2D Model** *Sokolov & Stone* June 1995
3. **Responses of Primary Production and Carbon Storage to Changes in Climate and Atmospheric CO_2 Concentration** *Xiao et al.* October 1995
4. **Application of the Probabilistic Collocation Method for an Uncertainty Analysis** *Webster et al.* January 1996
5. **World Energy Consumption and CO_2 Emissions: 1950-2050** *Schmalensee et al.* April 1996
6. **The MIT Emission Prediction and Policy Analysis (EPPA) Model** *Yang et al.* May 1996 (*superseded by No. 125*)
7. **Integrated Global System Model for Climate Policy Analysis** *Prinn et al.* June 1996 (*superseded by No. 124*)
8. **Relative Roles of Changes in CO_2 and Climate to Equilibrium Responses of Net Primary Production and Carbon Storage** *Xiao et al.* June 1996
9. **CO_2 Emissions Limits:** ***Economic Adjustments and the Distribution of Burdens*** *Jacoby et al.* July 1997
10. **Modeling the Emissions of N_2O and CH_4 from the Terrestrial Biosphere to the Atmosphere** *Liu* Aug. 1996
11. **Global Warming Projections:** ***Sensitivity to Deep Ocean Mixing*** *Sokolov & Stone* September 1996
12. **Net Primary Production of Ecosystems in China and its Equilibrium Responses to Climate Changes** *Xiao et al.* November 1996
13. **Greenhouse Policy Architectures and Institutions** *Schmalensee* November 1996
14. **What Does Stabilizing Greenhouse Gas Concentrations Mean?** *Jacoby et al.* November 1996
15. **Economic Assessment of CO_2 Capture and Disposal** *Eckaus et al.* December 1996
16. **What Drives Deforestation in the Brazilian Amazon?** *Pfaff* December 1996
17. **A Flexible Climate Model For Use In Integrated Assessments** *Sokolov & Stone* March 1997
18. **Transient Climate Change and Potential Croplands of the World in the 21st Century** *Xiao et al.* May 1997
19. **Joint Implementation:** ***Lessons from Title IV's Voluntary Compliance Programs*** *Atkeson* June 1997
20. **Parameterization of Urban Subgrid Scale Processes in Global Atm. Chemistry Models** *Calbo* et al. July 1997
21. **Needed: A Realistic Strategy for Global Warming** *Jacoby, Prinn & Schmalensee* August 1997
22. **Same Science, Differing Policies;** ***The Saga of Global Climate Change*** *Skolnikoff* August 1997
23. **Uncertainty in the Oceanic Heat and Carbon Uptake and their Impact on Climate Projections** *Sokolov et al.* September 1997
24. **A Global Interactive Chemistry and Climate Model** *Wang, Prinn & Sokolov* September 1997
25. **Interactions Among Emissions, Atmospheric Chemistry & Climate Change** *Wang & Prinn* Sept. 1997
26. **Necessary Conditions for Stabilization Agreements** *Yang & Jacoby* October 1997
27. **Annex I Differentiation Proposals:** ***Implications for Welfare, Equity and Policy*** *Reiner & Jacoby* Oct. 1997
28. **Transient Climate Change and Net Ecosystem Production of the Terrestrial Biosphere** *Xiao et al.* November 1997
29. **Analysis of CO_2 Emissions from Fossil Fuel in Korea: 1961–1994** *Choi* November 1997
30. **Uncertainty in Future Carbon Emissions:** ***A Preliminary Exploration*** *Webster* November 1997
31. **Beyond Emissions Paths:** ***Rethinking the Climate Impacts of Emissions Protocols*** *Webster & Reiner* November 1997
32. **Kyoto's Unfinished Business** *Jacoby et al.* June 1998
33. **Economic Development and the Structure of the Demand for Commercial Energy** *Judson et al.* April 1998
34. **Combined Effects of Anthropogenic Emissions and Resultant Climatic Changes on Atmospheric OH** *Wang & Prinn* April 1998
35. **Impact of Emissions, Chemistry, and Climate on Atmospheric Carbon Monoxide** *Wang & Prinn* April 1998
36. **Integrated Global System Model for Climate Policy Assessment:** ***Feedbacks and Sensitivity Studies*** *Prinn et al.* June 1998
37. **Quantifying the Uncertainty in Climate Predictions** *Webster & Sokolov* July 1998
38. **Sequential Climate Decisions Under Uncertainty:** ***An Integrated Framework*** *Valverde et al.* September 1998
39. **Uncertainty in Atmospheric CO_2 (Ocean Carbon Cycle Model Analysis)** *Holian* Oct. 1998 (*superseded by No. 80*)
40. **Analysis of Post-Kyoto CO_2 Emissions Trading Using Marginal Abatement Curves** *Ellerman & Decaux* Oct. 1998
41. **The Effects on Developing Countries of the Kyoto Protocol and CO_2 Emissions Trading** *Ellerman et al.* November 1998
42. **Obstacles to Global CO_2 Trading:** ***A Familiar Problem*** *Ellerman* November 1998
43. **The Uses and Misuses of Technology Development as a Component of Climate Policy** *Jacoby* November 1998
44. **Primary Aluminum Production:** ***Climate Policy, Emissions and Costs*** *Harnisch et al.* December 1998
45. **Multi-Gas Assessment of the Kyoto Protocol** *Reilly et al.* January 1999
46. **From Science to Policy:** ***The Science-Related Politics of Climate Change Policy in the U.S.*** *Skolnikoff* January 1999
47. **Constraining Uncertainties in Climate Models Using Climate Change Detection Techniques** *Forest et al.* April 1999
48. **Adjusting to Policy Expectations in Climate Change Modeling** *Shackley et al.* May 1999
49. **Toward a Useful Architecture for Climate Change Negotiations** *Jacoby et al.* May 1999
50. **A Study of the Effects of Natural Fertility, Weather and Productive Inputs in Chinese Agriculture** *Eckaus & Tso* July 1999
51. **Japanese Nuclear Power and the Kyoto Agreement** *Babiker, Reilly & Ellerman* August 1999
52. **Interactive Chemistry and Climate Models in Global Change Studies** *Wang & Prinn* September 1999
53. **Developing Country Effects of Kyoto-Type Emissions Restrictions** *Babiker & Jacoby* October 1999

Contact the Joint Program Office to request a copy. The Report Series is distributed at no charge.

105. **Analysis of Strategies of Companies under Carbon Constraint** *Hashimoto* January 2004
106. **Climate Prediction:** ***The Limits of Ocean Models*** *Stone* February 2004
107. **Informing Climate Policy Given Incommensurable Benefits Estimates** *Jacoby* February 2004
108. **Methane Fluxes Between Terrestrial Ecosystems and the Atmosphere at High Latitudes During the Past Century** *Zhuang et al.* March 2004
109. **Sensitivity of Climate to Diapycnal Diffusivity in the Ocean** *Dalan et al.* May 2004
110. **Stabilization and Global Climate Policy** *Sarofim et al.* July 2004
111. **Technology and Technical Change in the MIT EPPA Model** *Jacoby et al.* July 2004
112. **The Cost of Kyoto Protocol Targets:** ***The Case of Japan*** *Paltsev et al.* July 2004
113. **Economic Benefits of Air Pollution Regulation in the USA:** ***An Integrated Approach*** *Yang et al.* (revised) Jan. 2005
114. **The Role of Non-CO_2 Greenhouse Gases in Climate Policy:** ***Analysis Using the MIT IGSM*** *Reilly et al.* Aug. '04
115. **Future U.S. Energy Security Concerns** *Deutch* Sep. '04
116. **Explaining Long-Run Changes in the Energy Intensity of the U.S. Economy** *Sue Wing* Sept. 2004
117. **Modeling the Transport Sector:** ***The Role of Existing Fuel Taxes in Climate Policy*** *Paltsev et al.* November 2004
118. **Effects of Air Pollution Control on Climate** *Prinn et al.* January 2005
119. **Does Model Sensitivity to Changes in CO_2 Provide a Measure of Sensitivity to the Forcing of Different Nature?** *Sokolov* March 2005
120. **What Should the Government Do To Encourage Technical Change in the Energy Sector?** *Deutch* May '05
121. **Climate Change Taxes and Energy Efficiency in Japan** *Kasahara et al.* May 2005
122. **A 3D Ocean-Seaice-Carbon Cycle Model and its Coupling to a 2D Atmospheric Model:** ***Uses in Climate Change Studies*** *Dutkiewicz et al.* (revised) November 2005
123. **Simulating the Spatial Distribution of Population and Emissions to 2100** *Asadoorian* May 2005
124. **MIT Integrated Global System Model (IGSM) Version 2:** ***Model Description and Baseline Evaluation*** *Sokolov et al.* July 2005
125. **The MIT Emissions Prediction and Policy Analysis (EPPA) Model:** ***Version 4*** *Paltsev et al.* August 2005
126. **Estimated PDFs of Climate System Properties Including Natural and Anthropogenic Forcings** *Forest et al.* September 2005
127. **An Analysis of the European Emission Trading Scheme** *Reilly & Paltsev* October 2005
128. **Evaluating the Use of Ocean Models of Different Complexity in Climate Change Studies** *Sokolov et al.* November 2005
129. ***Future*** **Carbon Regulations and** ***Current*** **Investments in Alternative Coal-Fired Power Plant Designs** *Sekar et al.* December 2005
130. **Absolute vs. Intensity Limits for CO_2 Emission Control:** ***Performance Under Uncertainty*** *Sue Wing et al.* January 2006
131. **The Economic Impacts of Climate Change:** ***Evidence from Agricultural Profits and Random Fluctuations in Weather*** *Deschenes & Greenstone* January 2006
132. **The Value of Emissions Trading** *Webster et al.* Feb. 2006
133. **Estimating Probability Distributions from Complex Models with Bifurcations:** ***The Case of Ocean Circulation Collapse*** *Webster et al.* March 2006
134. **Directed Technical Change and Climate Policy** *Otto et al.* April 2006
135. **Modeling Climate Feedbacks to Energy Demand:** ***The Case of China*** *Asadoorian et al.* June 2006
136. **Bringing Transportation into a Cap-and-Trade Regime** *Ellerman, Jacoby & Zimmerman* June 2006
137. **Unemployment Effects of Climate Policy** *Babiker & Eckaus* July 2006
138. **Energy Conservation in the United States:** ***Understanding its Role in Climate Policy*** *Metcalf* Aug. '06
139. **Directed Technical Change and the Adoption of CO_2 Abatement Technology:** ***The Case of CO_2 Capture and Storage*** *Otto & Reilly* August 2006
140. **The Allocation of European Union Allowances:** ***Lessons, Unifying Themes and General Principles*** *Buchner et al.* October 2006
141. **Over-Allocation or Abatement?** ***A preliminary analysis of the EU ETS based on the 2006 emissions data*** *Ellerman & Buchner* December 2006
142. **Federal Tax Policy Towards Energy** *Metcalf* Jan. 2007
143. **Technical Change, Investment and Energy Intensity** *Kratena* March 2007
144. **Heavier Crude, Changing Demand for Petroleum Fuels, Regional Climate Policy, and the Location of Upgrading Capacity** *Reilly et al.* April 2007
145. **Biomass Energy and Competition for Land** *Reilly & Paltsev* April 2007
146. **Assessment of U.S. Cap-and-Trade Proposals** *Paltsev et al.* April 2007
147. **A Global Land System Framework for Integrated Climate-Change Assessments** *Schlosser et al.* May 2007
148. **Relative Roles of Climate Sensitivity and Forcing in Defining the Ocean Circulation Response to Climate Change** *Scott et al.* May 2007
149. **Global Economic Effects of Changes in Crops, Pasture, and Forests due to Changing Climate, CO_2 and Ozone** *Reilly et al.* May 2007
150. U.S. GHG Cap-and-Trade Proposals: ***Application of a Forward-Looking Computable General Equilibrium Model*** *Gurgel et al.* June 2007
151. Consequences of Considering Carbon/Nitrogen Interactions on the Feedbacks between Climate and the Terrestrial Carbon Cycle *Sokolov et al.* June 2007
152. Energy Scenarios for East Asia: 2005-2025 *Paltsev & Reilly* July 2007
153. Climate Change, Mortality, and Adaptation: ***Evidence from Annual Fluctuations in Weather in the U.S.*** *Deschênes & Greenstone* August 2007

Contact the Joint Program Office to request a copy. The Report Series is distributed at no charge.

Contact the Joint Program Office to request a copy. The Report Series is distributed at no charge.